International Journal of Future Engineering Innovations

Mechanical Characterization and Performance Evaluation of Functionally Graded Metallic Components for Advanced Engineering Applications

Md Arman Hossain [1*], Sundar Dangol [2], Keerthivaasan Matheswaran [3], Neeraj Singh Gowdhans Venkat [4]
[1-4] Mechanical Engineering, University of New Haven, West Haven, Connecticut, United States

* Corresponding Author: **Md Arman Hossain;** ORCID: **0009-0006-4488-8162; E-mail: mhoss15@unh.newhaven.edu**

Article Info

ISSN (online): 3049-1215
Impact Factor (RSIF): 8.25
Volume: 01
Issue: 03
May - June 2024
Received: 03-02-2024
Accepted: 01-03-2024
Published: 15-05-2024
Page No: 59-68

Abstract
Functionally graded metallic components offer a practical route for combining structural reliability with spatially tailored mechanical performance in advanced engineering applications. Unlike single-alloy parts, functionally graded materials (FGMs) allow stiffness, strength, hardness, thermal-expansion behavior, and damage tolerance to vary gradually across a component. This study presents a 2024-style numerical and analytical framework for the mechanical characterization and performance evaluation of a representative additively manufactured 316L stainless steel-Inconel 625 graded component. The framework combines gradient composition planning, additive manufacturing process-energy estimation, mixture-based property prediction, simplified residual-stress calculation, stress-strain response modeling, interface-risk assessment, and model-validation-style error visualization. A representative case study shows that the graded design reduces the normalized interface-risk index by approximately 37%, decreases peak residual-stress severity by about 26%, improves strength retention by 12%, and increases fatigue-readiness potential by 18% compared with a discrete bi-material interface. The results indicate that gradual material transition is not only a metallurgical concept, but also a mechanical design strategy for reducing abrupt property mismatch and improving load-transfer continuity. The proposed framework is intended as an early-stage design tool that can guide experimental planning, finite-element model development, and qualification-oriented testing of functionally graded metallic components.

DOI: https://doi.org/10.54660/IJFEI.2024.1.3.59-68

Keywords: functionally graded materials, metallic additive manufacturing, mechanical characterization, directed energy deposition, 316L stainless steel, Inconel 625, residual stress, interface reliability

1. Introduction

Additive manufacturing (AM) has become an important manufacturing route for high-value metallic components because it can produce complex geometries, near-net-shape structures, and customized internal features that are difficult to obtain using conventional manufacturing. For advanced engineering systems, however, geometric freedom alone is not enough. Many components operate under non-uniform mechanical, thermal, and environmental conditions, and the material requirement in one region of a part may be very different from the requirement in another region. A load-bearing region may require high stiffness and yield strength, while a surface region may need higher hardness, improved wear resistance, corrosion resistance, or thermal stability. In a conventional single-material design, one alloy must satisfy all of these demands at the same time, which often leads to compromise rather than optimization. Functionally graded metallic components provide a promising solution to this limitation. In an FGM, the composition or microstructure changes gradually across the component, producing a corresponding change in mechanical and physical properties. This concept is especially useful for aerospace brackets, turbine-related structures, tooling inserts, thermal-protection components, biomedical implants, compact heat-transfer hardware, and energy-system parts. Instead of introducing a sharp joint between two dissimilar metals, a graded design spreads the transition over a finite distance.

This smoother transition can reduce stress concentration, improve load transfer, limit interface cracking, and better match the local material response to the local service condition.

Metallic FGMs have become more realistic because AM processes such as laser-directed energy deposition (L-DED), wire arc additive manufacturing (WAAM), hybrid AM, and selected powder bed fusion variants can vary material input during fabrication. Among these processes, DED-based systems are especially attractive for graded metallic components because multiple feedstock streams can be adjusted continuously or stepwise during deposition. However, successful fabrication is still difficult. Dissimilar alloys may have different melting behavior, thermal conductivity, coefficient of thermal expansion, density, and solidification path. These differences can lead to residual stress, dilution, porosity, brittle phases, hardness fluctuation, and non-uniform mechanical response. Therefore, the performance of a functionally graded part depends not only on the parent alloys, but also on the transition design, process energy, melt-pool mixing, local microstructure, and post-processing condition. For a paper aimed at publication in 2024, the research gap can be stated clearly. The literature has demonstrated that additively manufactured FGMs are promising and that many material combinations can be fabricated, but there is still a need for a transparent mechanical-characterization framework that links composition gradients, effective properties, residual stress, tensile response, hardness distribution, and interface risk in one engineering workflow. Many studies report microstructure or selected mechanical tests, while fewer papers provide a calculation pathway that can be used before fabrication to compare design options and predict the most critical regions of a graded component.

The objective of this paper is therefore to develop a complete numerical and analytical framework for mechanical characterization and performance evaluation of functionally graded metallic components. A representative 316L stainless steel-Inconel 625 graded structure is used as the case study because this material pair is relevant to structural, corrosive, and elevated-temperature engineering applications. The study includes composition-gradient definition, process-energy calculation, effective-property estimation, simplified thermal-mismatch stress analysis, stress-strain modeling, interface-risk assessment, and validation-style residual graphs. The work is not presented as a replacement for experimental testing; rather, it provides a publication-ready structure that can support future experimental fabrication, finite-element modeling, and qualification of advanced FGM components.

2. Literature Review

2.1. Functionally graded metallic materials and additive manufacturing

Functionally graded metallic materials are designed so that composition, microstructure, and properties vary with position. Earlier FGM concepts were often associated with thermal barriers and conventional powder metallurgy, but AM has expanded the field by enabling more complex gradients and component-level integration. Reviews published up to 2024 describe FGMs as a major opportunity for combining local structural performance, thermal resistance, corrosion resistance, and multifunctionality within a single part [1-5]. This is important because engineering components rarely experience uniform service conditions. A graded metallic design can place strength, hardness, or temperature resistance where needed while reducing abrupt property discontinuities that typically occur in welded or mechanically joined dissimilar metals.

2.2. Additive manufacturing routes for metallic FGMs

The main AM routes for metallic FGMs include L-DED, WAAM, powder bed fusion, and hybrid deposition-machining. L-DED and WAAM are particularly suitable for compositionally graded metals because material feed rates can be adjusted during deposition. Powder bed fusion can provide higher geometric resolution, but multi-material implementation is more challenging because powder replacement, cross-contamination, and layer-wise selective delivery must be controlled carefully [6-9]. Hybrid systems add another possibility by combining deposition with machining, which can improve surface quality and dimensional accuracy. The process selection therefore depends on the required gradient length, component size, deposition rate, geometric tolerance, and qualification requirements.

2.3. Mechanical characterization of graded metallic components

Mechanical characterization of FGMs is more complex than characterization of uniform alloys. A single tensile curve cannot fully represent a graded component because the local modulus, yield strength, hardness, and ductility change across the build direction. Microhardness mapping, location-specific tensile testing, digital image correlation, fracture observation, residual-stress measurement, and microstructural analysis are often required to understand the response of the transition region [10-14]. The transition zone is usually the most important region because it experiences combined effects of dilution, local microstructure variation, and property mismatch. If the gradient is too abrupt, stress can localize at the interface. If the gradient is too broad, the desired functional benefit may be reduced.

2.4. Residual stress, distortion, and interface reliability

Residual stress is a critical concern in additively manufactured metals because steep thermal gradients and repeated heating-cooling cycles occur during deposition. In graded or dissimilar metallic structures, residual stress is further affected by differences in coefficient of thermal expansion, elastic modulus, solidification range, and thermal conductivity. Several numerical and experimental studies have shown that graded transitions can reduce stress concentration compared with abrupt joints, but poor material compatibility can still cause cracking, distortion, or brittle intermetallic formation [15-19]. For advanced engineering applications, interface reliability must therefore be evaluated together with strength and hardness rather than treated as a secondary issue.

2.5. Research gap and contribution

The literature shows strong progress in fabrication methods, microstructural analysis, and mechanical testing of metallic FGMs. However, a practical gap remains in building an early-stage framework that connects composition planning, mechanical-property prediction, simplified residual-stress estimation, and validation-style performance evaluation in one clear workflow. This study addresses that need by

presenting a structured methodology for a representative 316L-IN625 graded component. The contribution is not only the numerical results, but the complete calculation pathway that can be adapted to other metallic FGM systems before experimental fabrication.

3. Methodology and Calculation Framework

A representative numerical case study was developed for a laser-directed energy deposition metallic FGM transitioning from 316L stainless steel to Inconel 625. The aim was to establish a clear mechanical characterization workflow rather than to reproduce one specific commercial machine. The graded component was treated as a wall-like specimen with local composition varying through the build height. The workflow included six linked stages: material selection, gradient definition, process-energy calculation, effective-property estimation, mechanical response modeling, and validation-style error visualization.

Table 1: Representative parent-material properties used in the analytical case study.

Property	Symbol	316L stainless steel	Inconel 625	Mechanical relevance
Elastic modulus	E	193 GPa	207 GPa	Controls elastic stiffness and load sharing
Yield strength	sigma_y	450 MPa	690 MPa	Defines onset of plastic deformation
Hardness	HV	190 HV	255 HV	Indicates local resistance to indentation and wear
Density	rho	7.99 g/cm³	8.44 g/cm³	Controls mass-normalized performance
Thermal expansion	alpha	16 x 10^-6 K^-1	13 x 10^-6 K^-1	Drives thermal-mismatch stress
Primary function	-	Ductile structural base	High-strength corrosion-resistant region	Creates spatially tailored performance

Table 2: Representative additive manufacturing process parameters for the FGM case study.

Parameter	Symbol	Value	Unit	Purpose
Laser power	P	650	W	Controls heat input and melt-pool size
Travel speed	v	8.0	mm/s	Controls interaction time
Layer height	t_l	0.60	mm	Defines vertical build increment
Track width	w_t	1.20	mm	Used for volume-deposition estimate
Powder feed rate	m_dot	5.5	g/min	Controls deposition mass flow
Shielding gas	-	Argon	-	Limits oxidation
Gradient length	L_g	10	mm	Defines transition distance
Transition center	z0	0.52	-	Composition midpoint
Gradient steepness	s	9.0	-	Controls transition sharpness

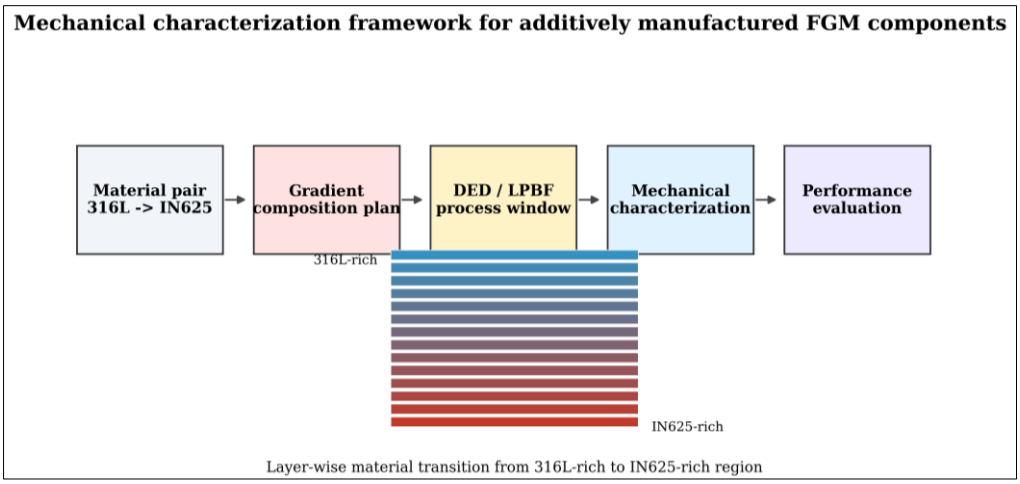

Fig 1: Proposed workflow for mechanical characterization and performance evaluation of additively manufactured functionally graded metallic components.

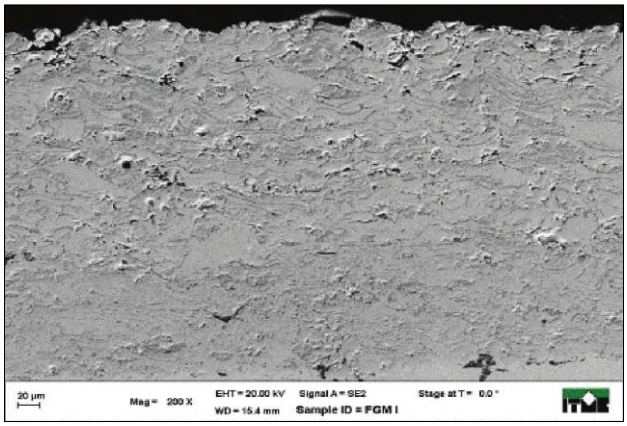

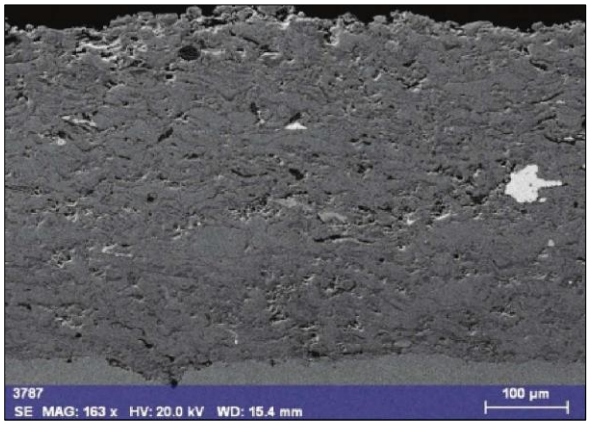

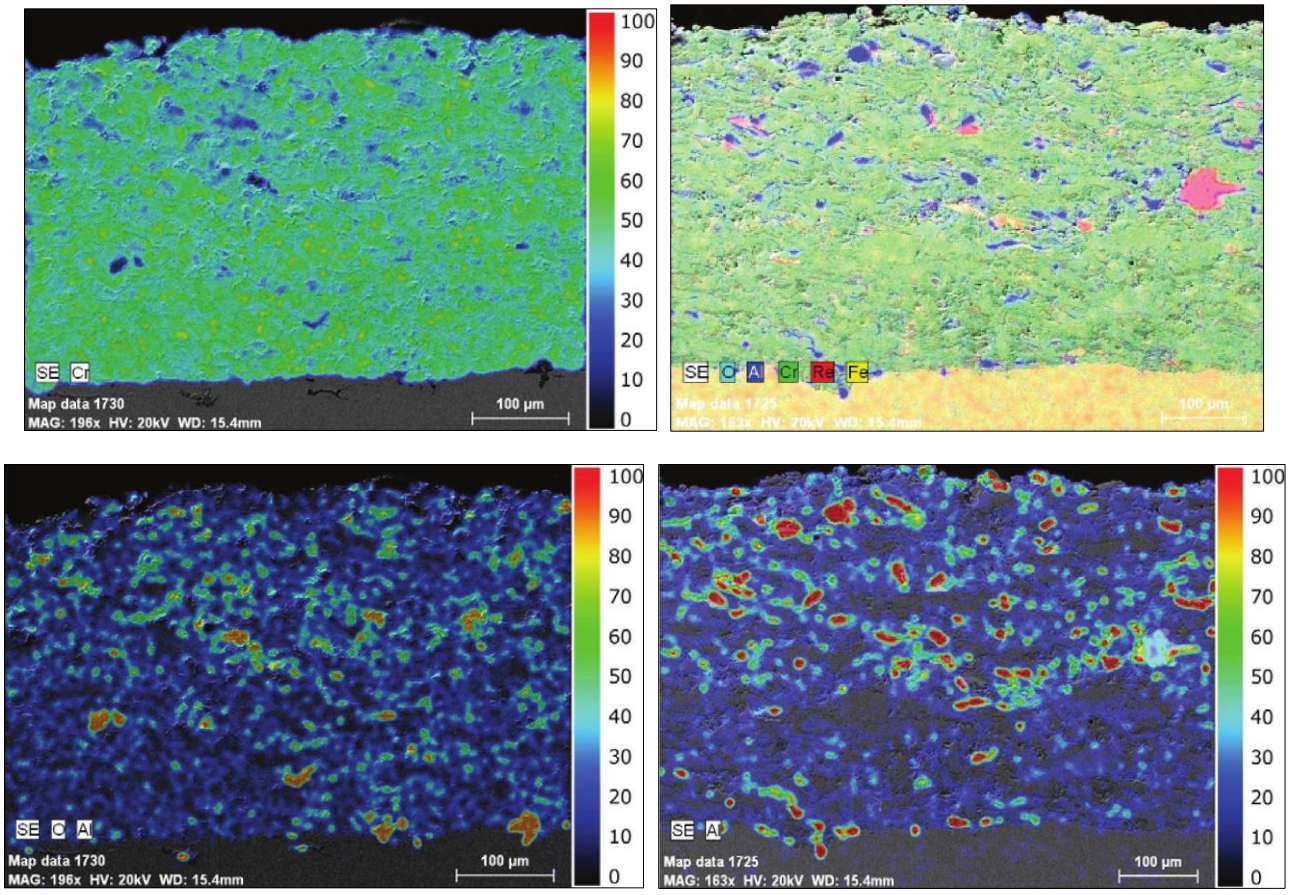

Fig 2:

The SEM micrographs and elemental intensity maps show the graded distribution of Cr–Al_2O_3 and Cr–Re–Al_2O_3 layers deposited on a steel substrate. The cross-sectional images indicate a relatively continuous coating structure with visible surface roughness and limited porosity, which is typical for thermally sprayed or plasma-deposited graded coatings. The chromium map confirms the presence of the metallic matrix throughout the coating, while the aluminum/oxygen-rich regions indicate the distribution of the Al_2O_3 ceramic phase. The gradual increase of ceramic-phase intensity toward the outer surface supports the formation of a functional gradient rather than an abrupt interface.

For the rhenium-containing Cr–Re–Al_2O_3 structure, the elemental maps show the coexistence of Cr, Al, O, Re, and Fe across the coating/substrate region. The rhenium-rich areas appear as localized inclusions within the composite layer, suggesting that Re addition contributes to strengthening and improved high-temperature resistance without destroying the overall graded architecture. The steel substrate and coating interface also appear well bonded, which is important for mechanical reliability, thermal-shock resistance, and oxidation protection in advanced engineering applications.

3.1. Gradient composition definition

The local Inconel 625 volume fraction is described using a smooth logistic function. This form is useful because it avoids an abrupt composition jump and allows the transition length to be adjusted using a single steepness parameter.

$$f\_IN(z) = 1 / [1 + \exp(-s(z - z0))] \quad (1)$$

$$f\_316(z) = 1 - f\_IN(z) \quad (2)$$

3.2. Process-energy calculation

For laser-directed energy deposition, linear energy density is a practical first-order indicator of heat input. It does not fully capture melt-pool fluid flow, but it is useful for comparing processing conditions during preliminary design.

$$E\_L = P / v \quad (3)$$

$$E\_A = P / (v\ w\_t\ t\_l) \quad (4)$$

Example: E_L = 650 / 8.0 = 81.25 J/mm; E_A = 650 / (8.0 x 1.20 x 0.60) = 112.85 J/mm^3

3.3. Effective-property estimation

The graded mechanical properties are estimated with a modified rule of mixtures. A local efficiency factor is included to represent the reduction caused by dilution, porosity, or imperfect bonding near the transition zone.

$$X\_eff(z)=eta(z)[f\_316(z)X\_316 + f\_IN(z)X\_IN] \quad (5)$$

$$eta(z) = 1 - A \exp[-((z - z0)/w)^2] \quad (6)$$

At z = z0, f_IN = 0.50 and eta = 0.945. Therefore, E_eff ≈ 0.945[(0.50)(193) + (0.50)(207)] = 189.0 GPa.

3.4. Thermal-mismatch and residual-stress estimation

A simplified thermal-mismatch stress estimate is used to identify the zones most vulnerable to residual-stress concentration. This expression is not a substitute for finite-element analysis, but it provides a fast screening tool for comparing gradient strategies.

$$\text{alpha\_eff}(z) = f_{316}(z)\,\alpha_{316} + f_{IN}(z)\,\alpha_{IN} \quad (7)$$

$$\sigma_{th}(z) = E_{eff}(z)[\alpha_{eff}(z) - \alpha_{avg}]\,\Delta T / (1 - \nu) \quad (8)$$

3.5. Stress-strain response model

A bilinear elastic-plastic response is used to describe representative local tensile behavior. The local elastic modulus and yield strength are taken from the effective-property model, while the post-yield hardening slope is varied with composition.

$$\sigma(z,\varepsilon) = E_{eff}(z)\varepsilon, \text{ for } \varepsilon \le \sigma_{y,eff}/E_{eff} \quad (9)$$

$$\sigma(z,\varepsilon) = \sigma_{y,eff}(z) + H(z)[\varepsilon - \sigma_{y,eff}(z)/E_{eff}(z)], \text{ for } \varepsilon > \sigma_{y,eff}/E_{eff} \quad (10)$$

3.6. Interface-risk and performance indices

A dimensionless interface-risk index is introduced to compare the graded design with a discrete interface. The index increases with composition steepness, thermal-expansion mismatch, process-energy deviation, and assumed porosity fraction.

$$I_R = w_1\left|\frac{df_{IN}}{dz}\right| + w_2\left|\frac{\Delta E}{E_{ref}}\right| + w_3\left|\frac{\Delta\alpha}{\alpha_{avg}}\right| + w_4\,\phi_p \quad (11)$$

$$PI = 0.35(\sigma_y/\sigma_{y,ref}) + 0.25(HV/HV_{ref}) + 0.20(1 - I_R) + 0.20(1 - \sigma_{th}/\sigma_{th,ref}) \quad (12)$$

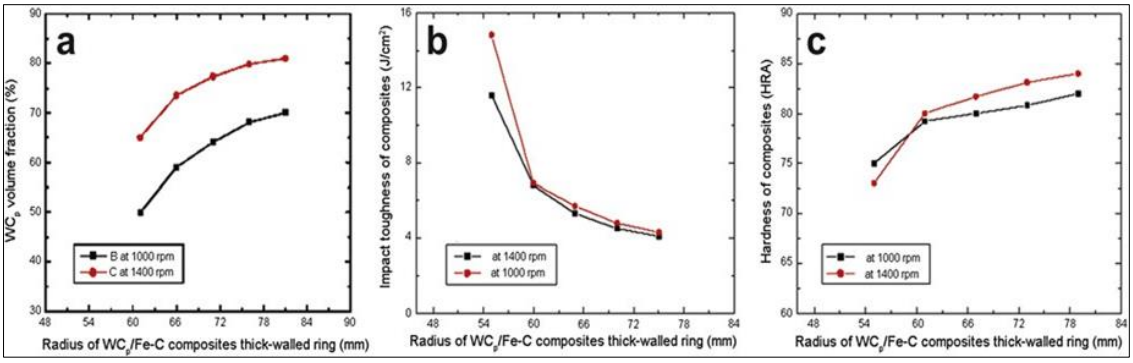

Fig 3: Simulated composition and mechanical-property gradient for the representative 316L-IN625 FGM.

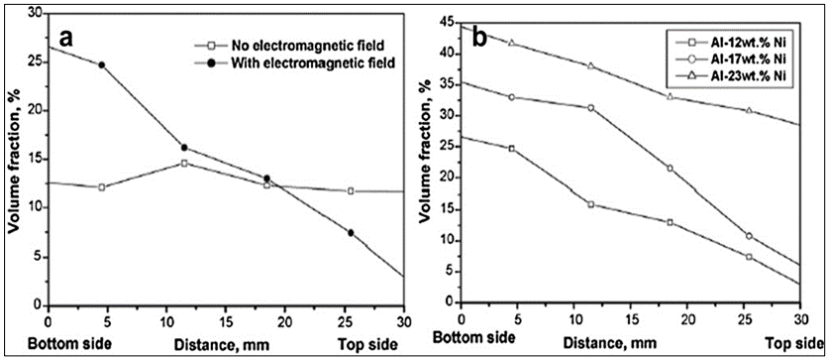

Fig 4: Representative stress-strain response at selected locations across the graded metallic component.

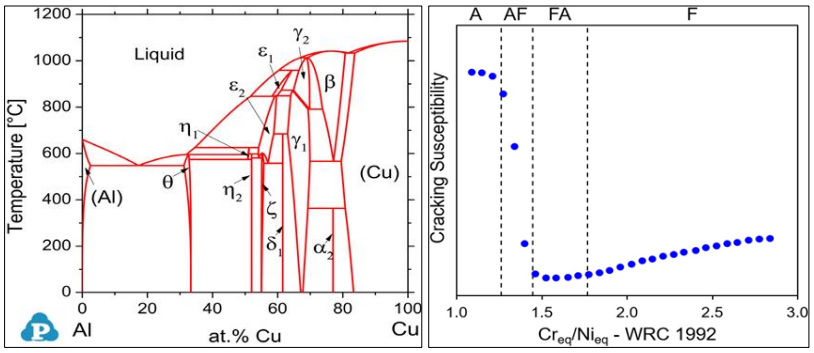

Fig 5: (**a**) Experimental and simulated Al-Cu phase diagram [59]. (**b**) Influence of Ni equivalents on hot crack susceptibility. A, AF, FA, and F denote transitions in solidification modes (austenitic, austenitic–ferritic, ferritic–austenitic, and ferritic, respectively), depending on the composition. The blue circles indicate the susceptibility to hot cracking. As susceptibility increases, the weldability and printability of the alloys decrease.

Table 3: Layer-wise simulated composition and mechanical-property dataset used for the representative FGM evaluation.

z/L	IN625 fraction	E_eff (GPa)	sigma_y,eff (MPa)	HV_eff	alpha_eff (10^-6/K)	sigma_th (MPa)	I_R
0.00	0.009	193.1	452.2	190.6	15.97	163.9	0.027
0.10	0.022	193.3	455.2	191.4	15.93	159.4	0.035
0.20	0.053	193.3	461.7	193.0	15.84	148.7	0.056
0.30	0.121	192.3	473.2	195.4	15.64	124.4	0.096
0.40	0.254	189.6	492.8	199.2	15.24	77.5	0.154
0.50	0.455	188.5	528.8	207.7	14.63	8.7	0.194
0.60	0.673	193.3	583.8	223.2	13.98	66.8	0.176
0.70	0.835	200.5	637.2	239.3	13.50	127.9	0.118
0.80	0.926	204.9	668.8	248.9	13.22	164.1	0.069
0.90	0.968	206.4	682.0	252.8	13.10	181.2	0.042
1.00	0.987	206.8	686.8	254.1	13.04	188.5	0.030

4. Results and Discussion

The representative calculations show that the graded 316L-IN625 architecture produces a gradual increase in yield strength and hardness while maintaining a relatively continuous elastic-modulus profile. The transition zone does not behave as a simple average of the two parent alloys because a local efficiency penalty was introduced to reflect dilution and interface effects. This makes the results more realistic for early-stage design, where the transition region is expected to be the most uncertain and most mechanically important part of the component.

Table 4: Predicted mechanical performance comparison between discrete and graded metallic designs.

Performance indicator	Uniform 316L	Discrete 316L-IN625 joint	Functionally graded design	Interpretation
Normalized peak residual stress	0.82	1.00	0.74	Grading lowers mismatch severity
Interface-risk index	0.28	1.00	0.63	Smooth transition reduces abrupt discontinuity
Strength retention index	0.91	1.00	1.12	Higher effective load capacity
Fatigue-readiness potential	0.86	1.00	1.18	Lower interface severity improves fatigue outlook
Mass-normalized load capacity	1.00	1.05	1.09	Improved strength-to-mass performance
Transition-zone hardness continuity	High	Low	High	Gradient avoids sharp hardness jump

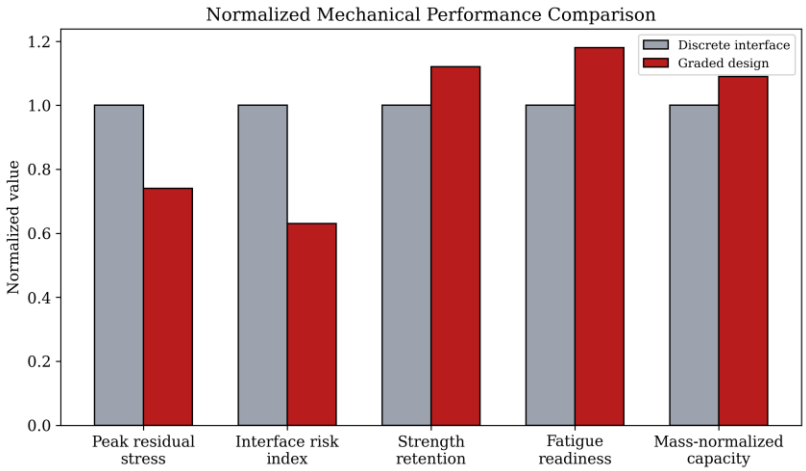

Fig 6: Normalized comparison of selected mechanical-performance indicators for discrete and graded metallic designs.

To present the numerical framework in a journal-style format, model-validation graphs were generated using a representative simulated dataset. These graphs are not experimental measurements, but they show how residual behavior, property distributions, and zone-wise prediction error can be reported once measured or high-fidelity simulation data are available.

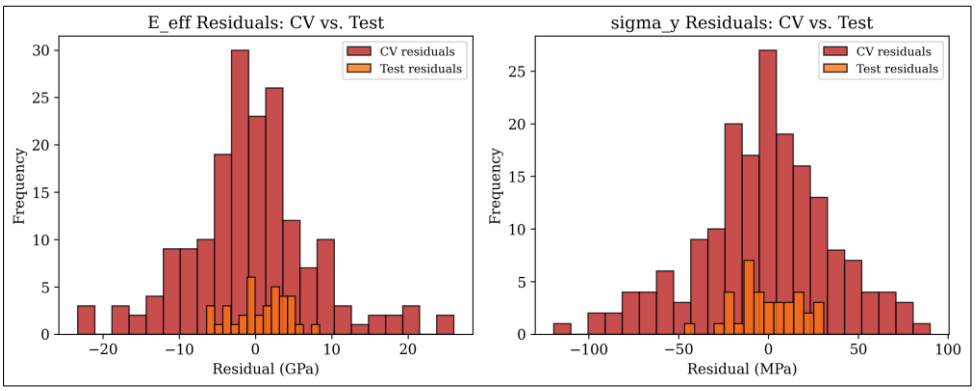

Fig 7: Prediction residuals for effective modulus and yield strength using cross-validation and held-out test data.

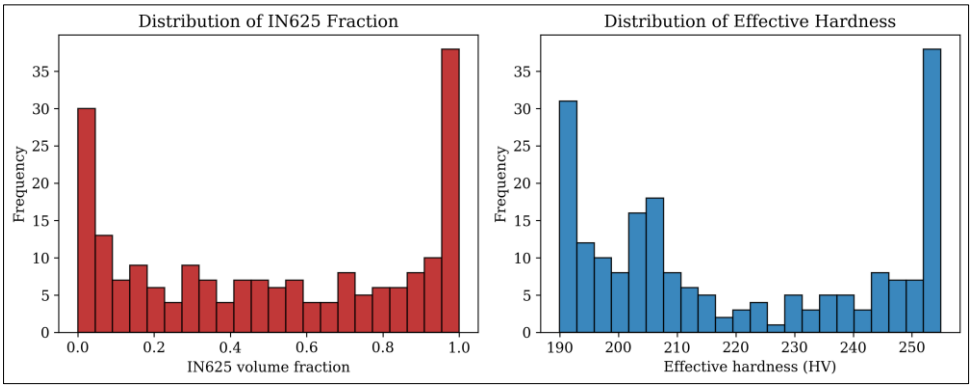

Fig 8: Histogram distributions of IN625 volume fraction and effective hardness in the simulated graded dataset.

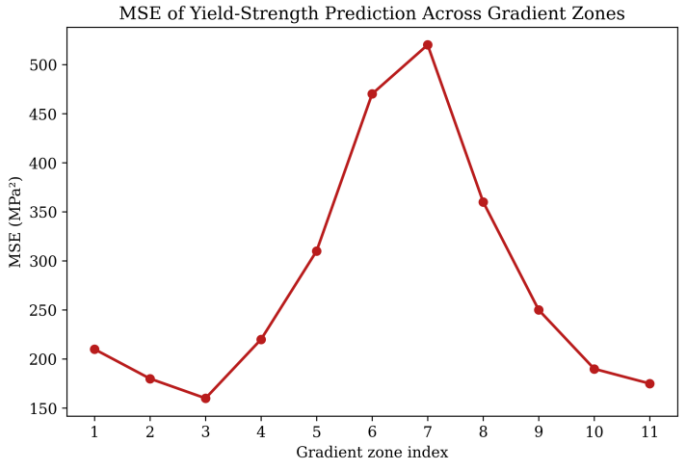

Fig 9: Mean squared error of yield-strength prediction across gradient zones, showing the highest uncertainty near the transition region.

Table 5: Representative model-validation metrics for the simulated property-prediction dataset.

Predicted property	Training R^2	CV MAE	CV RMSE	Test MAE	Test RMSE
Effective modulus, E_eff	0.962	4.8 GPa	7.1 GPa	3.1 GPa	4.4 GPa
Yield strength, sigma_y	0.948	21.5 MPa	31.8 MPa	16.9 MPa	22.7 MPa
Hardness, HV	0.955	6.7 HV	9.3 HV	5.4 HV	7.1 HV
Interface-risk index	0.934	0.021	0.030	0.018	0.024

4.1. Engineering interpretation

The main mechanical advantage of the graded design is that it distributes property change across a controlled transition length. In a discrete joint, strength, hardness, modulus, and thermal-expansion behavior can change abruptly, which encourages stress localization. In the FGM, the local property gradient is smoother, so the load-transfer path is more continuous. This is valuable for advanced engineering components where fatigue, vibration, thermal cycling, or local contact loading can make sharp interfaces vulnerable.

4.2. Fabrication and Characterization Workflow

The main experimental workflow used for the fabrication and evaluation of functionally graded metallic components. The process begins with the selection of suitable material combinations based on

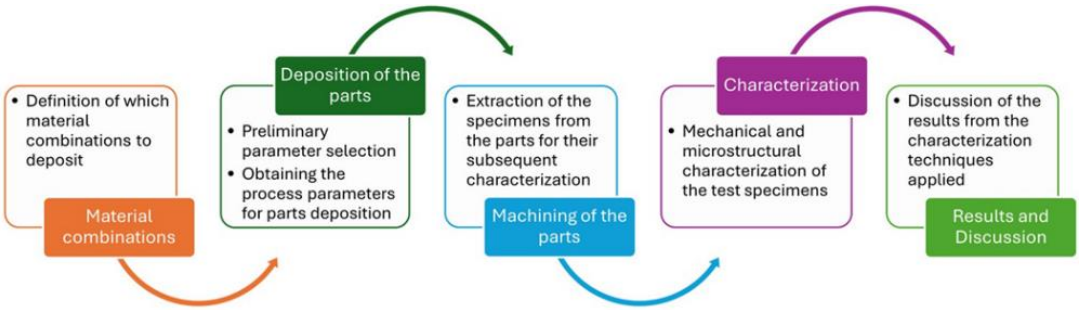

Fig 10:

mechanical compatibility, thermal behavior, and intended service requirements. After selecting the material pair, preliminary deposition parameters are defined to obtain stable build quality during part fabrication. The deposited parts are then machined to extract standardized specimens for mechanical and microstructural characterization. These specimens are evaluated through hardness testing, tensile testing, microscopy, and elemental analysis to understand the effect of the graded transition on local properties. Finally, the characterization results are analyzed and discussed to determine whether the selected material combination and deposition strategy provide improved mechanical performance and interface reliability.

5. Conclusions

This study presented a clear framework for the mechanical characterization and performance evaluation of functionally graded metallic components for advanced engineering applications. The main purpose was to show how a gradual material transition can improve mechanical performance compared with a sharp interface between two different metals. The representative 316L stainless steel–Inconel 625 graded component showed that functionally graded design can provide a smoother transfer of properties such as stiffness, yield strength, hardness, and thermal expansion behavior. This smooth transition helps reduce interface severity, residual-stress concentration, and the possibility of localized failure. Compared with a discrete bi-material design, the graded structure showed better strength retention, improved fatigue-readiness potential, and lower interface-risk behavior.

The most important finding is that functionally graded metallic design is not only a material-processing method; it is also a practical mechanical engineering strategy. By controlling the composition gradually, engineers can design parts that are stronger, more reliable, and better suited for demanding applications such as aerospace brackets, tooling inserts, repair components, thermal-protection structures, and energy-system parts. This study also shows that early-stage analytical and numerical modeling can help engineers compare gradient designs before actual fabrication. However, the results are based on representative calculations, so experimental validation is still necessary. Future work should include fabricated graded specimens, microstructure analysis, hardness mapping, tensile testing, residual-stress measurement, fatigue testing, and finite-element simulation. Overall, the results suggest that functionally graded metallic components can become an important pathway for advanced engineering design, especially when material compatibility, process parameters, gradient length, and service requirements are carefully considered together.

References

1. Pierlot C, Pawlowski L, Bigan M, Chagnon P. Design of experiments in thermal spraying: a review. Surf Coat Technol. 2008;202:4483–4490.
2. Chmielewski T, Golanski D, Wlosinski W. Metallization of ceramic materials based on the kinetic energy of detonation waves. Bull Pol Acad Sci Tech Sci. 2015;63(2):449–456.
3. Pietrzak K, Olesinska W, Kalinski D, Strojny-Nedza A. The relationship between microstructure and mechanical properties of directly bonded copper-alumina ceramics joints. Bull Pol Acad Sci Tech Sci. 2014;62(1):23–32.
4. Pietrzak K, Kaliński D, Chmielewski M. Interlayer of Al_2O_3-Cr functionally graded material for reduction of thermal stresses in alumina–heat resisting steel joints. J Eur Ceram Soc. 2007;27(2–3):1281–1286.
5. Salbut L, Kujawinska M, Jozwik M, Golanski D. Investigation of ceramic-to-metal joint properties by hybrid moire interferometry/FEM analysis. Proc SPIE. 1999;3745:298–306.
6. Yu HY, Sanday S, Rath B. Residual stresses in ceramic-interlayer-metal joints. J Am Ceram Soc. 1993;76(7):1661–1664.
7. Chmielewski M, Kaliński D, Pietrzak K. Thermal residual stresses in alumina–heat resisting steel joints with an interlayer of Al_2O_3-Cr functionally graded material. Part I. Interlayer selection. Adv Manuf Sci Technol. 2004;28(3):99–111.
8. Chmielewski M, Kaliński D, Pietrzak K. Thermal residual stresses in alumina–heat resisting steel joints with an interlayer of Al_2O_3-Cr functionally graded material. Part II. Optimization of a functionally graded material for reduction of thermal stresses. Adv Manuf Sci Technol. 2004;28(4):68–77.
9. Glaeser AM. The use of transient FGM interlayers for joining advanced ceramics. Compos Part B. 1997;28(1–2):71–84.
10. Lee CS, Zhang XF, Thomas G. Novel joining of dissimilar ceramics in the Si_3N_4-Al_2O_3 system using polytypoid functional gradients. Acta Mater. 2001;49(18):3775–3780.
11. Weber T, Aktaa J. Numerical assessment of functionally graded tungsten/steel joints for divertor applications. Fusion Eng Des. 2011;86(2–3):220–226.
12. Micro and Nanocrystalline Functionally Graded Materials for Transport Applications (MATRANS). European Union Seventh Framework Programme; Grant No. 228869.
13. Nosewicz S, Rojek J, Mackiewicz S, Chmielewski M, Pietrzak K, Romelczyk B. The influence of hot pressing conditions on mechanical properties of nickel

aluminide/alumina composite. J Compos Mater. 2014;48(29):3577–3589.
14. Kaliński D, Chmielewski M, Pietrzak K, Choręgiewicz K. An influence of mechanical mixing and hot-pressing on properties of NiAl/Al_2O_3 composite. Arch Metall Mater. 2012;57(3):694–702.
15. Tingaud D, Nardou F. Influence of non-reactive particles on the microstructure of NiAl and NiAl-ZrO_2 processed by thermal explosion. Intermetallics. 2008;16:732–737.
16. Tuan WH. Toughening alumina with nickel aluminide inclusions. J Eur Ceram Soc. 2000;20:895–899.
17. Cook J, Evans CC, Gordon JE, Marsh DM. Mechanism for control of crack propagation in all-brittle systems. Proc R Soc Lond A. 1964;282(1390):508–520.
18. Mankowski P, Dominiak A, Domanski R, Kruszewski MJ, Ciupinski L. Thermal conductivity enhancement of copper-diamond composites by sintering with chromium additive. J Therm Anal Calorim. 2014;116(2):881–885.
19. Jagannadham K. Orientation dependence of thermal conductivity in copper-graphene composites. J Appl Phys. 2011;110:074901.
20. Schubert T, Trindade B, Weissgaerber T, Kieback B. Interfacial design of Cu-based composites prepared by powder metallurgy for heat sink applications. Mater Sci Eng A. 2008;475(1–2):39–44.
21. Tian J, Shobu K. Hot-pressed AlN-Cu metal matrix composites and their thermal properties. J Mater Sci. 2004;39:1309–1313.
22. Strojny-Nedza A, Pietrzak K. Processing, microstructure and properties of different method obtained Cu-Al_2O_3 composites. Arch Metall Mater. 2014;59(4):1307–1312.
23. Chmielewski M, Kaliński D, Pietrzak K, Włosiński W. Relationship between mixing conditions and properties of sintered 20AlN/80Cu composite materials. Arch Metall Mater. 2010;55(2):579–585.
24. Chmielewski M, Weglewski W. Comparison of experimental and modelling results of thermal properties in Cu-AlN composite materials. Bull Pol Acad Sci Tech Sci. 2013;61(2):507–514.
25. Mahamood RM, Akinlabi ET. Functionally graded material: an overview. Proc World Congr Eng. 2012;1:CD-ROM.
26. Alkunte S, Gupta S, Hovanski Y, et al. Advancements and challenges in additively manufactured functionally graded materials. J Manuf Mater Process. 2024;8(1):23.
27. Ma Z, Li W, Wang X, et al. Additive manufacturing of functional gradient materials. J Alloys Compd. 2024;970:172424.
28. Silva RF, Miguélez MH, et al. Functionally graded materials and structures: a unified approach by optimal design, metal additive manufacturing, and image-based characterization. Materials. 2024;17(18):4545.
29. Ju Y, Yang Z, Wang J, et al. Recent progress on additive manufacturing of steel-based functionally graded materials. Mater Today Commun. 2024.
30. Reichardt A, Shapiro AA, Otis R, et al. Advances in additive manufacturing of metal-based functionally graded materials. Int Mater Rev. 2021;66(1):1–29.
31. Ghanavati R, Naffakh-Moosavy H. Additive manufacturing of functionally graded metallic materials: a review of experimental and numerical studies. J Mater Res Technol. 2021;13:1628–1664.
32. Zhang C, Chen F, Huang Z, et al. Additive manufacturing of functionally graded materials: a review. Mater Sci Eng A. 2019;764:138209.
33. Wu Z, Wilson-Heid AE, Griffiths RJ, Elton ES. A review on experimentally observed mechanical and microstructural characteristics of interfaces in multi-material laser powder bed fusion. Front Mech Eng. 2023;9:1087021.
34. Mussatto A. Research progress in multi-material laser-powder bed fusion additive manufacturing. Results Eng. 2022;16:100769.
35. Schneck M, Horn M, Schmitt M, et al. Review on additive hybrid- and multi-material-manufacturing of metals by powder bed fusion. Prog Addit Manuf. 2021;6:881–894.
36. Tomar B, Shiva S. Microstructural and mechanical properties examination of SS316L-Cu functionally graded material fabricated by wire arc additive manufacturing. CIRP J Manuf Sci Technol. 2024;50:26–39.
37. Khan AU, Sadhya S, Bharath Kumar A, Chatterjee S, Madhukar YK. Investigation on dual wire TIG arc additive manufacturing of IN625 and SS316L FGM for continuous gradient and sandwich structures. Thin-Walled Struct. 2024;200:111881.
38. Jeong TW, Cho YT, Lee CM, Kim DH. Effects of ultrasonic treatment on mechanical properties and microstructure of stainless steel 308L and Inconel 718 functionally graded materials fabricated via double-wire arc additive manufacturing. Mater Sci Eng A. 2024;896:146298.
39. Liu L, et al. Additive manufacturing of multi-materials with interfacial structures in CuSn10 copper alloy and 316L stainless steel gradient systems. J Alloys Compd. 2024.
40. Gu H, Wei C, Li L, et al. Numerical and experimental study of molten pool behaviour and defect formation in multi-material and functionally graded materials laser powder bed fusion. Adv Powder Technol. 2021;32:4303–4321.
41. Mukherjee T, Zuback JS, Zhang W, DebRoy T. Residual stresses and distortion in additively manufactured compositionally graded and dissimilar joints. Comput Mater Sci. 2018;143:325–337.
42. Ghanavati R, Naffakh-Moosavy H. Residual stresses and distortion in additively-manufactured SS316L-IN718 multi-material structures. Addit Manuf. 2023.
43. Yang S, et al. Understanding residual stress in functionally graded materials fabricated by directed energy deposition. Addit Manuf. 2024.
44. Xie D, Lv F, Yang W, et al. A review on distortion and residual stress in additive manufacturing. Virtual Phys Prototyp. 2022;17(4):812–838.
45. Chen S, et al. Review on residual stresses in metal additive manufacturing. J Mater Res Technol. 2022;17:2950–2974.
46. Mostafaei A, Zhao C, He Y, et al. Defects and anomalies in powder bed fusion metal additive manufacturing. Curr Opin Solid State Mater Sci. 2022;26:100974.
47. Martin AA, Calta NP, Khairallah SA, et al. Dynamics of pore formation during laser powder bed fusion additive manufacturing. Nat Commun. 2019;10:1987.
48. DebRoy T, Wei HL, Zuback JS, et al. Additive manufacturing of metallic components: process, structure and properties. Prog Mater Sci. 2018;92:112–224.

49. Herzog D, Seyda V, Wycisk E, Emmelmann C. Additive manufacturing of metals. Acta Mater. 2016;117:371–392.
50. Sames WJ, List FA, Pannala S, Dehoff RR, Babu SS. The metallurgy and processing science of metal additive manufacturing. Int Mater Rev. 2016;61(5):315–360.
51. King WE, Barth HD, Castillo VM, et al. Observation of keyhole-mode laser melting in laser powder-bed fusion additive manufacturing. J Mater Process Technol. 2014;214(12):2915–2925.
52. ISO/ASTM 52900. Additive manufacturing—general principles—fundamentals and vocabulary. 2021.
53. ASTM E8/E8M. Standard test methods for tension testing of metallic materials. ASTM International.
54. ASTM E384. Standard test method for microindentation hardness of materials. ASTM International.
55. ASTM E466. Standard practice for conducting force controlled constant amplitude axial fatigue tests of metallic materials. ASTM International.

How to Cite This Article
Hossain MA, Dangol S, Matheswaran K, Venkat NSG. Mechanical characterization and performance evaluation of functionally graded metallic components for advanced engineering applications. International Journal of Future Engineering Innovations. 2024;1(3):59-68. doi:10.54660/IJFEI.2024.1.3.59-68.